


# Targeting CDK9 and MCL-1 by a new CDK9/p-TEFb inhibitor with and without 5-fluorouracil in esophageal adenocarcinoma

Zhimin Tong\*, Alicia Mejia\*, Omkara Veeranki, Anuj Verma, Arlene M. Correa, Rashmi Dokey, Viren Patel, Luisa Maren Solis, Barbara Mino, Riham Kathkuda, Jaime Rodriguez-Canales, Steven H. Lin, Sunil Krishnan, Scott Kopetz, Mariela Blum, Jaffer A. Ajani, Wayne L. Hofstetter and Dipen M. Maru 

## Abstract

**Background:** CDK9 inhibitors are antitumorigenic against solid tumors, including esophageal adenocarcinoma (EAC). However, efficacy of a CDK9 inhibitor combined with 5-fluorouracil (5-FU) and target proteins that are targeted by these agents in EAC are unknown.

**Methods:** The anti-EAC efficacy of a new CDK9 inhibitor, BAY1143572, with and without 5-FU was assessed *in vitro* and in xenograft models in athymic nu/nu mice. Synergy between BAY1143572 and 5-FU in inhibiting cell proliferation was analyzed by calculating the combination index using CompuSyn software. Potential targets of BAY1143572 and 5-FU were identified by reverse-phase protein array. The effects of BAY1143572 and 5-FU on MCL-1 *in vitro* were analyzed by Western blotting, quantitative real-time polymerase chain reaction, and chromatin immunoprecipitation assay. MCL-1 protein expression in tumors from patients with locoregional EAC treated with chemoradiation and surgery was assessed by immunohistochemistry.

**Results:** BAY1143572 had dose-dependent antiproliferative and proapoptotic effects and demonstrated synergy with 5-FU against EAC *in vitro*. The median volumes of FLO-1 and ESO-26 xenografts treated with 5-FU plus BAY114352 were significantly smaller than those of xenografts treated with either agent alone ( $p < 0.05$ ). BAY1143572 downregulated MCL-1 by inhibiting HIF-1 $\alpha$  binding to the MCL-1 promoter. 5-FU enhanced BAY1143572-induced MCL-1 downregulation and stable MCL-1 overexpression reduced the apoptosis induced by BAY1143572 and 5-FU *in vitro*. High patients' tumor MCL-1 expression was correlated with shorter overall and recurrence-free survival.

**Conclusions:** BAY1143572 and 5-FU have synergistic antitumorigenic effects against EAC. MCL-1 is a downstream target of CDK9 inhibitors and a predictor of response to neoadjuvant chemoradiation in EAC.

**Keywords:** adenocarcinoma, CDK9, 5-fluorouracil and MCL-1, esophagus

Received: 20 October 2018; revised manuscript accepted: 16 June 2019.

## Introduction

Preoperative chemotherapy or chemoradiation followed by surgery have improved survival outcomes and the likelihood of margin-negative esophagogastrectomy in patients with locoregional esophageal

adenocarcinoma (EAC).<sup>1</sup> However, these patients' 5-year survival rates remain low.<sup>2,3</sup> Biomarker-driven targeted therapies have had limited success in EAC patients, primarily in less than 20% of those with stage IV human epidermal growth factor

*Ther Adv Med Oncol*

2019, Vol. 11: 1–17

DOI: 10.1177/  
1758835919864850

© The Author(s), 2019.  
Article reuse guidelines:  
[sagepub.com/journals-](https://sagepub.com/journals-permissions)  
permissions

Correspondence to:

**Dipen M. Maru**  
Division of Pathology and  
Laboratory Medicine,  
Unit 085, The University  
of Texas MD Anderson  
Cancer Center, 1515  
Holcombe Blvd., Houston,  
TX, 77030, USA.  
[dmaru@mdanderson.org](mailto:dmaru@mdanderson.org)

**Zhimin Tong**  
**Alicia Mejia**  
**Omkara Veeranki**  
**Rashmi Dokey**  
**Viren Patel**  
Department of Pathology,  
The University of Texas MD  
Anderson Cancer Center,  
Houston, TX, USA

**Anuj Verma**  
**Luisa Maren Solis**  
**Barbara Mino**  
**Riham Kathkuda**  
**Jaime Rodriguez-Canales**  
Department of  
Translational Molecular  
Pathology, The University  
of Texas MD Anderson  
Cancer Center, Houston,  
TX, USA

**Arlene M. Correa**  
**Wayne L. Hofstetter**  
Department of Thoracic  
and Cardiovascular  
Surgery, The University  
of Texas MD Anderson  
Cancer Center, Houston,  
TX, USA

**Steven H. Lin**  
**Sunil Krishnan**  
Department of Radiation  
Oncology, The University  
of Texas MD Anderson  
Cancer Center, Houston,  
TX, USA

**Scott Kopetz**  
**Mariela Blum**  
**Jaffer A. Ajani**  
Department of  
Gastrointestinal Medical  
Oncology, The University  
of Texas MD Anderson  
Cancer Center, Houston,  
TX, USA

\*These authors contributed  
equally to the study.

receptor 2 (Her2-neu)-overexpressing disease who receive trastuzumab.<sup>4-6</sup> To date, no targeted agent has demonstrated benefit as an adjunct to 5-fluorouracil-based chemotherapy or chemoradiation in patients with locally advanced EAC.

EAC, but not normal esophageal squamous epithelium or Barrett esophagus, overexpresses cyclin-dependent kinase 9 (CDK9), an evolutionarily conserved ubiquitous serine threonine kinase.<sup>7</sup> CDK9 is a transcriptional CDK and an essential component of positive transcription elongation factor b (p-TEFb). p-TEFb, which phosphorylates the carboxy terminal of RNA polymerase II, prolongs the transcription of proteins with short half-lives, such as myeloid cell leukemia-1 (MCL-1). MCL-1 and other CDK9-regulated proteins play important roles in several cellular processes critical to oncogenesis. Some of these processes, such as apoptosis, are enhanced by CDK9 inhibition and chemotherapy. CDK9 inhibitors and chemotherapeutic agents, owing to their common cellular mechanism, very likely have synergy against tumors.<sup>8-10</sup>

In phase I/II trials, CDK9 inhibitors elicited limited treatment responses and had high toxicity in patients with solid tumors.<sup>11-16</sup> These drugs' low efficacy is partly due to their lack of specificity against CDK9. Therefore, demonstration of target specificity against CDK 9 is important in improving efficacy of the CDK9 inhibitors. In one recent study, we demonstrated the efficacy of two CDK inhibitors with predominant CDK9 inhibitory effects in *in vitro* and xenograft models of EAC; we also demonstrated that CDK9 downregulation by shRNA (shCDK9) and treatment with a CDK inhibitor reduces the phosphorylation of RNA polymerase II at serine 2, a CDK9-specific function, and downregulates common CDK9 targets such as MCL-1 and c-Myc in EAC.<sup>7</sup> These findings indicate that CDK9 inhibitors have on target effects against CDK9 in EAC.

One novel first-in-class CDK9-specific inhibitor, BAY1143572 (Atuveciclib), potently inhibits CDK9 (p-TEFb) activity; its effect against CDK9 is more than 50-fold greater than that against other CDKs. One recent study showed that BAY1143572 inhibits pSer2 and pSer7 RNA Pol II, as well as MYC and MCL-1, and induces apoptosis in adult T-cell leukemia and lymphoma.<sup>17,18</sup> In preclinical models of solid tumors, BAY1143572 at nanomolar doses had antitumor activity without any off-target effects, indicating

its high specificity for CDK9.<sup>19</sup> Recently, we have demonstrated radiation-sensitizing effects of BAY1143572 in preclinical models of EAC (manuscript under review). However, whether BAY1143572 or any other CDK9 inhibitor have a role as an adjuvant to chemotherapy for EAC is not known.

In this study, we assessed the synergy between BAY1143572 and 5-fluorouracil in suppressing tumor growth and downregulating MCL-1 in *in vitro* and xenograft models of EAC. *In vivo* experiments were performed with murine xenografts because of ability to test the efficacy and toxicity of a drug against intact tumor and normal tissue in these models. Experiments with xenograft models generate robust preclinical data, an essential step before proceeding to a human clinical trial. Furthermore, we also studied the prognostic relevance of tumor cell MCL-1 expression in patients with locoregional EAC treated with neoadjuvant chemoradiation (including 5-fluorouracil) and esophagogastrectomy. By these experiments, we have tested a hypothesis that BAY1143572 and 5-fluorouracil have synergistic antitumorigenic properties against EAC and MCL-1 is a shared target of these two agents.

### Material and methods

The study was approved by MD Anderson's Institutional Review Board (PA15-0887 and LAB04-0979, PI: DMM). The requirement for informed consent was waived because all samples were from residual tissue in blocks generated for standard-of-care pathology processing and no additional sampling from patients was required. All experiments involving laboratory animals were approved by MD Anderson's Institutional Animal Care and Use Committee (IACUC-1155-RN01, PI: DMM) and performed in accordance with the guidelines mandated by the Public Health Service Policy on Humane Care and Use of Laboratory Animals.

### Cell cultures and reagents

BAY1143572 was purchased from Active Biochemical (Wan Chai, Hong Kong). 5-fluorouracil and the human EAC cell lines OE33, FLO-1, and SKGT4 were purchased from Sigma-Aldrich (St. Louis, MO). OE19, SKGT2, and ESO-26 cells were obtained from Dr. Steven H. Lin (MD Anderson Cancer Center). OE33, OE19, SKGT2, and ESO-26 cells were maintained in RPMI

medium containing 2mM L-glutamine and 10% fetal bovine serum (FBS). FLO-1 and SKGT4 cells were maintained in Dulbecco's modified Eagle's medium (DMEM) containing 10% FBS. 293FT cells were obtained from Invitrogen (Carlsbad, CA) and maintained in DMEM supplemented with 10% FBS and 500µg/ml G418. All cell lines were maintained in a 5% CO<sub>2</sub> atmosphere at 37°C and passaged at 80% confluence using 0.05% trypsin–ethylenediaminetetraacetic acid for 3–5 min.

#### *Cell proliferation assay*

Cell proliferation after treatment with vehicle (control) only, with 5-fluorouracil and/or BAY1143572 was measured using an MTS assay (Cell Titer Aqueous One Solution Cell Proliferation Assay, Promega, Madison, WI). Briefly, cells were incubated with the reaction solution containing MTS reagent for 1 h at 37°C. The absorbance at 490nm was measured using a microplate reader. The results are presented as values normalized to the control. The experiment was performed in triplicate for each treatment condition. The half maximal inhibitory concentration (IC<sub>50</sub>) values for BAY1143572 were calculated with an equation derived from a best-fit dose–response curve created in Microsoft Excel.

The synergism between BAY1143572 and 5-fluorouracil in inhibiting cell proliferation was analyzed by calculating combination index (CI) values using CompuSyn software.<sup>20,21</sup> The CI is a quantitative measure based on the mass-action law of the degree of drug interaction in terms of synergism and antagonism for a given endpoint of the measured effect. A CI value of less than 0.1 indicates very strong synergism; 0.1–0.3, strong synergism; 0.3–0.7, synergism; 0.7–0.85, moderate synergism; 0.85–0.90, slight synergism; 0.9–1.10, nearly additive; and higher than 1.10, antagonism.<sup>22,23</sup>

#### *Cell apoptosis*

EAC cells were treated with vehicle only, 5-fluorouracil and/or BAY1143572; washed with cold phosphate-buffered saline, resuspended in 100µl of binding buffer containing 5µl of recombinant Annexin V–fluorescein isothiocyanate (FITC, BD Biosciences, San Jose, CA) and 10µl of a 50µg/ml propidium iodide solution, and then incubated for 15 min at room temperature. The percentage of cells undergoing apoptosis in each

treatment cohort was analyzed by flow cytometry at MD Anderson's Flow Cytometry and Cellular Imaging Facility. The experiments were performed in triplicate for each treatment condition.

#### *Reverse phase protein array*

Cell lysates were prepared and serially diluted twofold for five dilutions (from undiluted to a 1:16 dilution). The diluted lysates were then arrayed on nitrocellulose-coated slides in an 11 × 11 format, probed with antibodies by tyramide-based signal amplification, and visualized by 3, 3'-diaminobenzidine colorimetric reaction. The slides were scanned on a flatbed scanner to produce 16-bit TIFF images. Spots on the TIFF images were identified, and the staining density was quantified using the Array-Pro Analyzer software program (Meyer Instruments, Houston, TX). Relative protein levels for each sample were determined by interpolating each dilution curve from the 'standard curve' (supercurve) of the antibody. Protein-level data were normalized for protein loading and transformed to linear values.<sup>24,25</sup> The linear values were compared across the treatment cohorts, and linear values of treatment group(s) that were 0.1 higher or lower than those of controls were considered to identify upregulated and downregulated proteins, respectively.

#### *Western blotting*

For each sample, the total protein was separated by 8% or 10% sodium dodecyl sulfate–polyacrylamide gel electrophoresis and transferred onto polyvinylidene fluoride transfer membranes (GE Healthcare Life Sciences, Pittsburgh, PA). Antibodies against MCL-1 (Santa Cruz Biotechnology, Santa Cruz, CA) and phosphorylated RNA polymerase II CTD (pSer2; Novus Biologicals, Littleton, CO) were used for immunoblotting of MCL-1 and pSer2 proteins. Bands were visualized by enhanced chemiluminescence detection (GE Healthcare Life Sciences). The experiments were performed in triplicate for each treatment condition.

#### *Quantitative real-time polymerase chain reaction*

For quantitative real-time polymerase chain reaction (qPCR), 0.5µg of total RNA isolated from cells treated with vehicle only, with BAY1143572 and/or 5-fluorouracil were reverse-transcribed to cDNA using SuperScript II Reverse Transcriptase

(Invitrogen). qPCR was performed with the QuantiFast SYBR Green PCR kit (Qiagen, Valencia, CA) on a Life Technologies instrument. PCR primers were designed using the primer3 program according to the DNA sequence of MCL-1. qPCR was performed in triplicate for each treatment condition. The  $C_t$  value of GAPDH was subtracted from that of MCL-1 to obtain a  $\Delta C_t$  value. The  $\Delta C_t$  value of the control was subtracted from the  $\Delta C_t$  value of each treated sample to obtain a  $\Delta\Delta C_t$  value. The MCL-1 expression levels of the experimental groups relative to those of the controls were expressed as  $2^{-\Delta\Delta C_t}$ . All experiments were performed in triplicate.

#### *Chromatin immunoprecipitation assay*

Chromatin immunoprecipitation (ChIP) assay was performed using the Pierce Agarose ChIP Kit (Thermo Scientific, Rockford, IL). Briefly, cells were treated with  $1\mu\text{M}$  BAY1143572 or control vehicle for 4h and then fixed with 1% formaldehyde to cross-link DNA and protein. The chromatin was digested with micrococcal nuclease to obtain chromatin fragments of 200–1000bp. Ten per cent of the chromatin fragments were used as input DNA. The immunoprecipitation was performed with either an anti-HIF-1 $\alpha$  antibody or an immunoglobulin G control (Cell Signaling Technology). The immunoprecipitated DNA was then quantitated using real-time PCR with specific primers for the MCL-1 promoter (forward: 5'-AGGTCACCTTGAGGCCATGAG-3'; reverse: 5'-CACGTTTCAGACGATTCGGTA-3'). These primers cover the -1051 to -901bp region of the MCL-1 promoter. The enrichment of targeted genomic regions was normalized with input DNA and presented as a value relative to the immunoglobulin G control.

#### *Lentivirus generation and stable overexpression of MCL-1 in EAC cell lines*

Human MCL-1 cDNA was released from the pCMV-SPORT6 (OriGene Technologies Inc., Rockville, MD) vector with the EcoRI enzyme and subcloned into the lentiviral vector pCDH-VMV-MCS-EF1-Puro (Addgene, Cambridge, MA) between EcoRI to create a pHMCL-1 vector. The identity and orientation of this construct were confirmed by DNA sequencing. To produce an MCL-1-overexpressing lentivirus, we cotransfected pHMCL-1 and control vectors with their packaging and envelope plasmids into 293FT cells using Lipofectamine 2000 Transfection

Reagent (Invitrogen) according to the manufacturer's instructions. The viral supernatant was collected 48h after transfection and centrifuged at 3000rpm for 15min to remove debris. For transduction with the lentivirus, cells were infected with  $2\times$  diluted virus media containing  $6\mu\text{g/ml}$  polybrene for 16h. Cells stably overexpressing MCL-1 were selected by incubation in a puromycin-containing medium for at least 2 weeks. Target protein expression was confirmed by Western blotting.

#### *EAC xenograft studies*

The animals were provided by Jackson Laboratories (MD, USA) or Experimental Radiation Oncology, MD Anderson Cancer Center. All xenografts experiments were performed with 4- to 6-week-old female athymic nu/nu mice, whose mean weight was 20g (range, 17–22g). All mice were treatment naïve and did not undergo any genetic manipulation. We chose athymic nu/nu mice because these immunodeficient rodents cannot reject implanted tumor and the rate of tumor growth in these models is predictable. Female mice were used because of timely availability of the female athymic nu/nu mice as compared with male mice. All laboratory animals were kept in modified barrier housing. All animals had social housing and environmental enrichment in accordance with the current edition of the Guide for the Care and Use of Laboratory Animals and the Animal Welfare Act.

BAY1143572 (7.5mg/ml) and 5-fluorouracil (10mg/ml) were dissolved in DMSO (vehicle) to generate injectable formulations. To identify the effective dose of BAY1143572, we subcutaneously injected  $4.5\times 10^6$  FLO-1 cells into the right flanks of the mice. Once the tumors reached 5mm in diameter, the mice were randomly divided into three treatment cohorts of seven mice each: (1) a control cohort treated with vehicle only; (2) a cohort treated with 12.5mg/kg BAY1143572; and (3) a cohort treated with 15mg/kg BAY1143572. Vehicle alone or BAY1143572 were given daily (in the morning) by intraperitoneal injection for 10 days under isoflurane vaporizer anesthesia. Isoflurane vaporizers are traditional anesthetic systems that allow proper, safe, and effective delivery of inhalant anesthetic agent to rodents.

To assess the synergistic effect of BAY1143572 and 5-fluorouracil in inhibiting the growth of EAC

xenografts, we randomly divided FLO-1 xenograft-bearing mice into six cohorts of seven to nine mice each: (1) a control cohort treated with vehicle only; (2) a cohort treated with 12.5 mg/kg BAY1143572; (3) a cohort treated with 15 mg/kg BAY1143572; (4) a cohort treated with 20 mg/kg 5-fluorouracil; (5) a cohort treated with 12.5 mg/kg BAY1143572 plus 20 mg/kg 5-fluorouracil; and (6) a cohort treated with 15 mg/kg BAY1143572 plus 20 mg/kg 5-fluorouracil. ESO-26 xenograft-bearing mice were randomly divided into four cohorts of seven to nine mice each: (1) a control cohort treated with vehicle only; (2) a cohort treated with 15 mg/kg BAY1143572; (3) a cohort treated with 20 mg/kg 5-fluorouracil; and (4) a cohort treated with 15 mg/kg BAY1143572 plus 20 mg/kg 5-fluorouracil. For all xenograft experiments, BAY1143572 was given daily (in the morning) for 10 days and 5-fluorouracil (in the morning) was given every 3 days for 2 weeks; both agents were given by intraperitoneal injection. The number of mice for the cohorts was decided based on our prior studies.

The xenografts were measured with digital calipers every 3 days. The xenograft volume was calculated as  $(W^2 \times L)/2$ , where  $W$  is the small diameter of the tumor and  $L$  is the large diameter of the tumor. In FLO-1 and ESO-26 bearing xenografts experiments, mice were weighed every other day and monitored daily for toxicity signs such as respiratory distress, gastrointestinal toxicity, intra-abdominal fluid collection, ruffled fur, hunched posture, and reduced food intake and for moribund signs such as impaired ambulation, muscular atrophy, lethargy, bleeding, central nervous system disturbances, and inability to remain upright. All laboratory animals were humanely killed by CO<sub>2</sub> asphyxiation when tumors reached the maximum size allowed as per the Institutional Animal Care and Use Committee guidelines or at the end of the experiment. The personnel who humanely killed the mice were adequately trained and used methods that are consistent with American Veterinary Medical Association Guidelines for the Euthanasia of Animals.

#### *MCL-1 immunohistochemistry analysis in tumor samples from EAC patients*

MCL-1 immunohistochemistry was performed on formalin-fixed, paraffin-embedded tissue sections of pretreatment tumor samples from 63 patients with locoregional EAC who were treated with neoadjuvant chemoradiation followed by esophagogastrectomy at MD Anderson. The neoadjuvant chemoradiation regimens included

fluoropyrimidine-based (plus taxol and/or platinum) chemotherapy and radiation in 59 patients and taxol and/or platinum (without fluoropyrimidine) and radiation in four patients. The clinical and pathologic features of these patients are listed in Supplementary Table 2. For immunohistochemistry, the slides were stained with rabbit monoclonal anti-MCL-1 antibody, clone D5V5L (Cell Signaling Technology, cat. #39224) using a Leica Bond Max automated stainer (Leica Biosystems Nussloch GmbH, Nußloch, Germany). Antigen retrieval was performed with Bond Solution #2 (Leica Biosystems), equivalent to ethylenediaminetetraacetic acid buffer pH 9.0, for 20 min followed by staining with a 1:100 dilution of the primary antibody for 20 min at room temperature. The primary antibody was detected using the Bond Polymer Refine Detection Kit (Leica Biosystems) with diaminobenzidine as the chromogen. Tumor cells with cytoplasmic staining intensity scores of 0, 1, 2, or 3 were manually counted at 200× magnification by a pathologist (AV), who was blinded to the patients' preclinical data and clinicopathologic features. The *H*-score for the cytoplasmic immunostaining of MCL-1 was calculated as the percentage of cells with intensity 0 × 0 + the percentage of cells with intensity 1 × 1 + the percentage of cells with intensity 2 × 2 + the percentage of cells with intensity 3 × 3. Tumors with *H*-scores lower than the median *H*-score were classified as having low MCL-1 expression, and tumors with *H*-scores equal to or higher than the median *H*-score were classified as having high MCL-1 expression.

#### *Statistical analysis*

*In vitro* data are the means ± the standard error (SE) from three independent experiments. For *in vitro* and xenografts assays, Student's *t* test was used to assess differences between groups. Patient demographics, clinical and pathologic information, and survival data were obtained from hospital charts and the hospital tumor registry. The Chi-squared or Fisher exact *t* test was used to compare categorical data. The prognostic significance of clinical and pathologic characteristics and MCL-1 *H*-score in relation to overall survival was assessed using univariate Cox regression analysis. Cox proportional hazards models were fitted for the multivariate analysis. After interactions between variables had been examined, a backward stepwise procedure was used to derive the best-fitting model. The statistical analysis was

conducted using the SPSS software program (SPSS, Chicago, IL). Kaplan–Meier survival curves were drawn with GraphPad Prism (version 4 for Windows; GraphPad Software, San Diego, CA).  $p$  values  $\leq 0.05$  were considered significant.

## Results

### *BAY1143572 is cytotoxic to EAC in vitro and in xenografts*

BAY1143572 at doses within a narrow  $IC_{50}$  range (0.73–1.95  $\mu\text{M}$ ) had a dose-dependent antiproliferative effect in six EAC cell lines (Figure 1A). Compared with control cells, cells treated with BAY1143572 at a dose within the same narrow  $IC_{50}$  range had higher rates of apoptosis in four of six cell lines; BAY1143572 increased apoptosis by a median of 20% in FLO-1 cells and 5% in SKGT2, SKGT4, and OE19 cells. The increases in apoptosis after treatment with BAY1143572 in OE33 and ESO26 cells were not statistically significant (Figure 1B). Compared with control, 12.5 or 15 mg/kg BAY1143572 reduced FLO-1 xenograft growth by 44% and 61%, respectively (Figure 1C). Mice did not lose weight or show significant signs of toxicity or morbidity throughout the treatment period (Figure 1D).

### *Synergy between BAY1143572 and 5-fluorouracil in in vitro models of EAC*

Compared with vehicle, 1.5  $\mu\text{M}$  BAY1143572 plus 10  $\mu\text{M}$  5-fluorouracil had a very strong synergistic antiproliferative effect in OE33 cells, resulting in an 80% reduction in proliferation (CI, 0.048); 2  $\mu\text{M}$  BAY1143572 plus 5  $\mu\text{M}$  5-fluorouracil had a strong synergistic antiproliferative effect in FLO-1 cells, resulting in a 67% reduction in proliferation (CI, 0.674); and 1  $\mu\text{M}$  BAY1143572 plus 10  $\mu\text{M}$  5-fluorouracil had a moderate synergistic antiproliferative effect in SKGT4 cells (CI, 0.83) (Figure 2A). In FLO-1 and SKGT4 cells, BAY1143572 plus 5-fluorouracil induced more apoptosis than that achieved with either agent alone (Figure 2B). In FLO-1 cells, 1  $\mu\text{M}$  BAY1143572 (a dose lower than the  $IC_{50}$ ) plus 5  $\mu\text{M}$  5-fluorouracil achieved 20% more apoptosis than BAY1143572 alone did and 25% more apoptosis than 5-fluorouracil alone did. In SKGT4 cells, 5  $\mu\text{M}$  BAY1143572 plus 10  $\mu\text{M}$  5-fluorouracil achieved 10% more apoptosis than BAY1143572 alone did and 35% more apoptosis than 5-fluorouracil alone did (Figure 2B). In OE33 cells, BAY1143572 plus

5-fluorouracil did not induce significantly more apoptosis than that induced by either agent alone.

### *BAY1143572 enhances the effects of 5-fluorouracil in murine xenografts of EAC*

Treatment with 20 mg/kg 5-fluorouracil every 3 days for 2 weeks shrunk FLO-1 xenografts in three mice and slowed xenograft growth in six mice 40 days after treatment initiation. The median xenograft volume of the cohort treated with 5-fluorouracil was 31% smaller than that of the cohort treated with vehicle only. Treatment with 12.5 mg/kg BAY1143572 daily for 10 days shrunk xenografts in three mice and slowed xenograft growth in five mice 40 days after treatment initiation. The median xenograft volume of the cohort treated with 12.5 mg/kg BAY1143572 was 39% smaller than that of the cohort treated with vehicle only. Treatment with 15 mg/kg BAY1143572 daily for 10 days shrunk xenografts in four mice and slowed xenograft growth in four mice 40 days after treatment initiation. The median xenograft volume of the cohort treated with 12.5 mg/kg BAY1143572 was 35% smaller than that of the cohort treated with 5-fluorouracil.

The median xenograft volume of the cohort treated with 15 mg/kg BAY1143572 was 36% smaller than that of the cohort treated with vehicle only. Treatment with 12.5 mg/kg BAY1143572 daily for 10 days plus 20 mg/kg 5-fluorouracil every 3 days for 2 weeks shrunk xenografts in six mice and markedly slowed xenograft growth in one mouse. The median xenograft volume of the cohort treated with 12.5 mg/kg BAY1143572 plus 5-fluorouracil was 65% smaller than that of the cohort treated with 5-fluorouracil alone and 13% smaller than that of the cohort treated with 12.5 mg/kg BAY1143572 alone. Treatment with 15 mg/kg BAY1143572 daily for 10 days plus 20 mg/kg 5-fluorouracil every 3 days for 2 weeks shrunk xenografts in three mice and markedly slowed xenograft growth in five mice. The median xenograft volume of the cohort treated with 15 mg/kg BAY1143572 plus 5-fluorouracil was 94% smaller than that of the cohort treated with 5-fluorouracil alone and 83% smaller than that of the cohort treated with 15 mg/kg BAY1143572 alone (Figure 2C).

The mean ESO-26 xenograft volumes of the cohorts treated with BAY1143572 alone or BAY1143572 plus 5-fluorouracil were 46% and 65% smaller, respectively, than that of the cohort

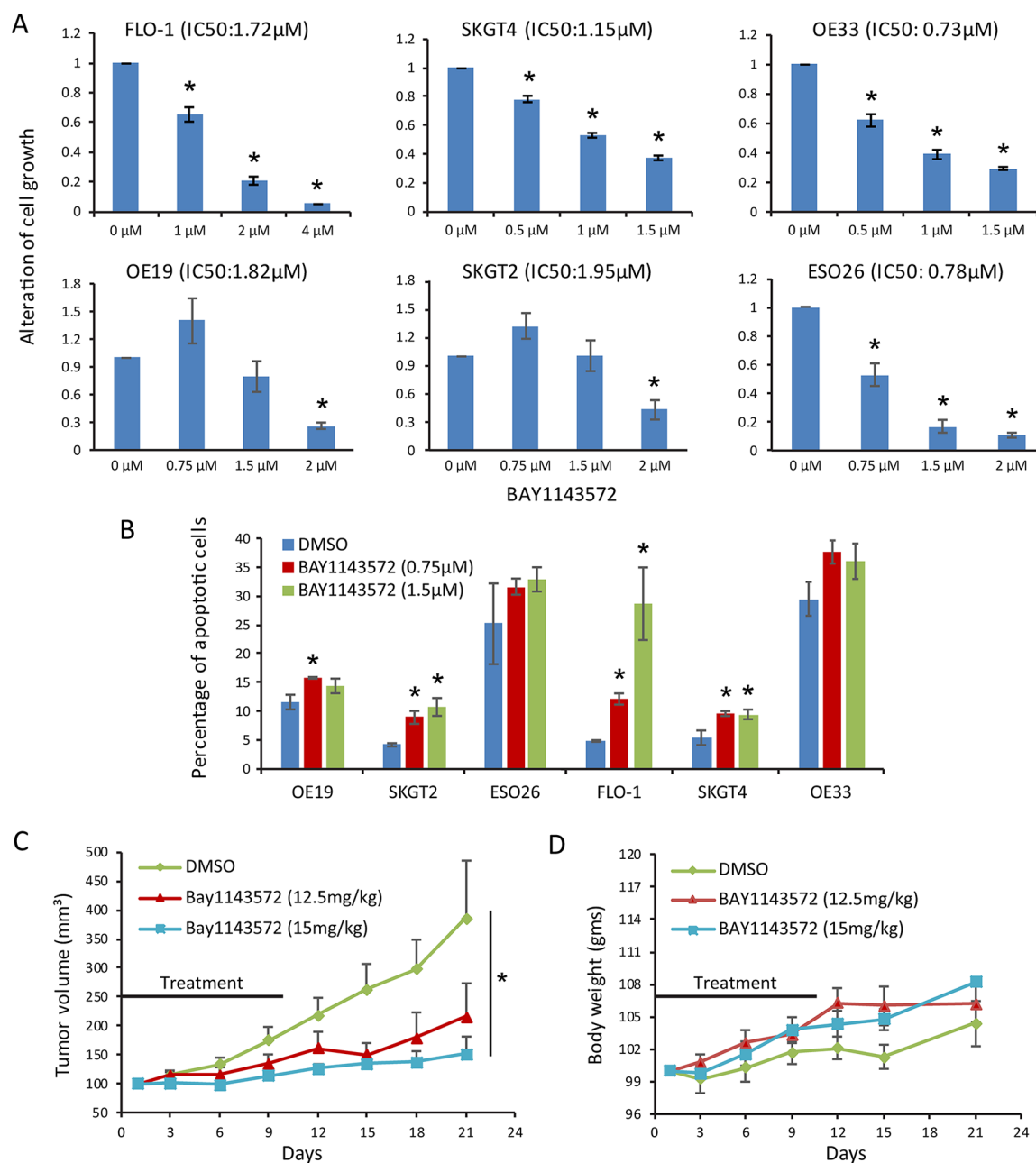


**Figure 1. BAY1143572 is an effective cytotoxic agent *in vitro* and *in vivo*.** Esophageal adenocarcinoma cells were treated with BAY1143572 at the indicated doses for 48h and then assessed for cell proliferation by MTS assay (A) and for apoptosis by flow cytometry (B). (C) Xenograft-bearing mice were treated with vehicle (DMSO) or with 12.5 or 15 mg/kg BAY1143572 by intraperitoneal injection daily for 10 days. Data are the mean percentages of tumor growth  $\pm$  SE. \* $p < 0.05$  compared with untreated controls. (D) Body weight chart of the xenograft-bearing mice treated with vehicle or with 12.5 or 15 mg/kg BAY1143572.

treated with vehicle only. In addition, the mean xenograft volume of the cohort treated with BAY1143572 plus 5-fluorouracil was 55% smaller than that of the cohort treated with 5-fluorouracil alone and 33% smaller than that of the cohort treated with BAY1143572 alone (Figure 2C).

Xenograft-bearing mice treated with 15 mg/kg BAY114372 plus 5-fluorouracil had significant weight loss during the treatment period but were able to gain weight after the treatment was stopped. No other signs of toxicity were observed in any treatment group.

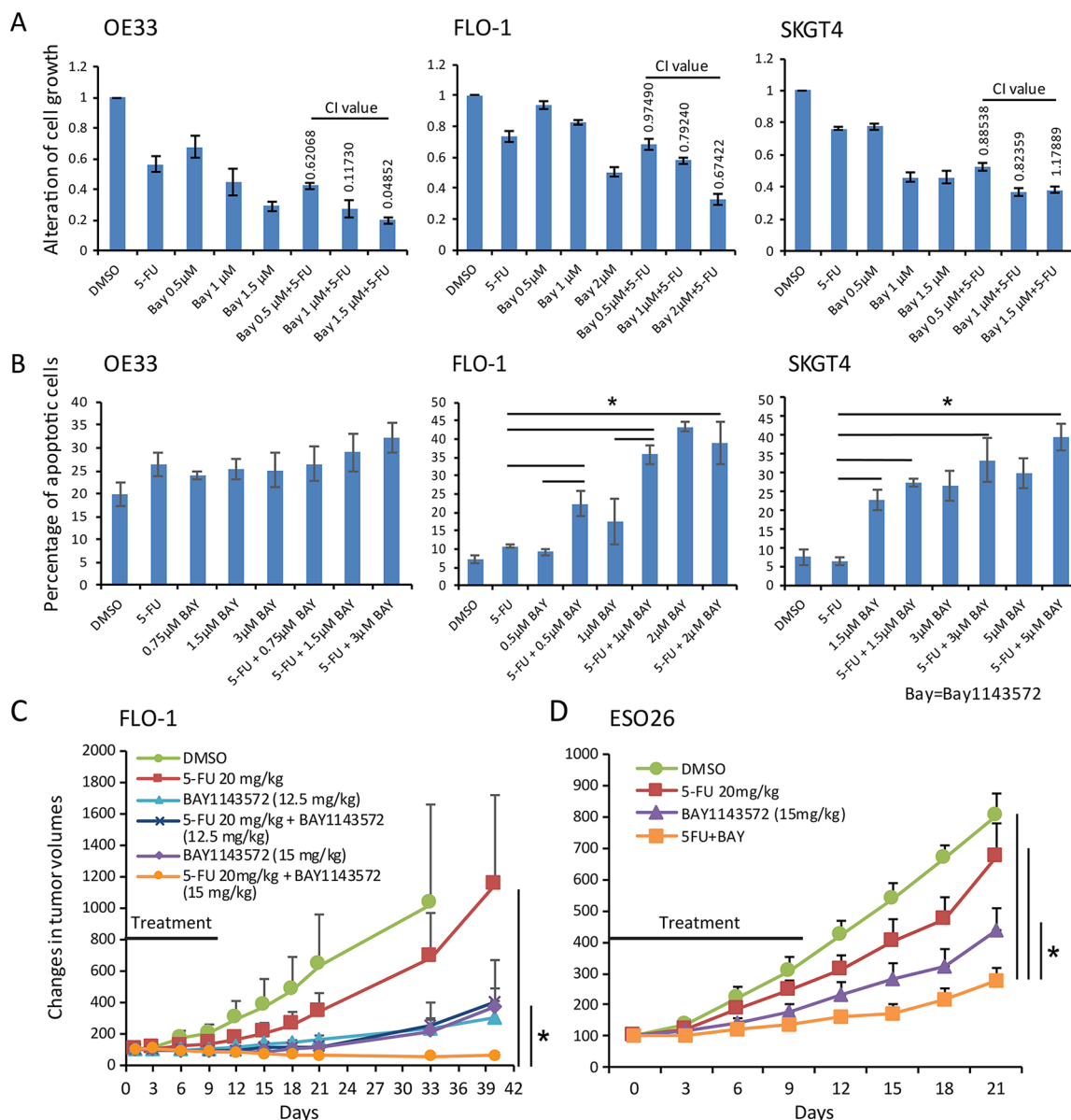


**Figure 2. BAY1143572 and 5-fluorouracil synergistically inhibit esophageal adenocarcinoma *in vitro* and in murine xenografts.** (A) Cells pretreated with 5-fluorouracil (5 μM for FLO-1 cells, 10 μM for OE33 and SKGT4 cells) for 24 h were treated with BAY1143572 at the indicated doses for 48 h and then analyzed for cell proliferation by MTS assay. Data are the means ± standard error (SE) of three independent experiments. (B) Cells treated with BAY1143572 with or without 5-fluorouracil were stained with Annexin V-FITC and propidium iodide. Apoptosis was determined by flow cytometry. Data are the means ± SE of 3 independent experiments. \**p* < 0.05. (C) and (D) The xenograft-bearing mice were treated with BAY1143572 (12.5 or 15 mg/kg for FLO-1 xenografts, 15 mg/kg for ESO-26 xenografts) daily for 10 days and/or 20 mg/kg 5-fluorouracil every 3 days for 2 weeks by intraperitoneal injection. Tumor growth was measured as tumor volume. Data are the percentages of tumor growth. \**p* < 0.05.

*Effects of BAY1143572 with and without 5-fluorouracil on MCL-1 in EAC in vitro*  
Reverse phase protein array (RPPA) analysis of FLO-1, OE33, and SKGT4 cells revealed that in two of three EAC cell lines, treatment

with 5-fluorouracil or BAY1143572 upregulated oncoproteins that included ATMpS1981, a post-translational form of ATM in response to DNA damage repair; BCL2 and cyclin-B1, regulators of the G2M phase of the cell cycle; FOX-M1, a



regulator of DNA damage repair; GATA3, an inducer of epithelial differentiation; MERIT40pS29; and elongation factor Tu, mitochondrial (TUFM; Supplementary Table 1 and Figure 3). Treatment with 5-fluorouracil plus BAY1143572 enhanced the upregulation of ATMpS1981, cyclin-B1, FOX-M1, MERIT40pS29, and TUFM.

In two of three EAC cell lines, treatment with 5-fluorouracil or BAY1143572 downregulated several oncoproteins, including ACCpS79, beta-actin, CDC25C (a regulator of transition from G2M to S phase), DUSP4, eF2K, human epidermal growth factor receptor 2, HES1, hexokinase II, IGF2BP2, LRP6pS1490 (a Wnt pathway receptor), MCL-1 (a critical protein in apoptotic pathways), MNK1, PMS2, and SCD. Treatment with 5-fluorouracil and BAY1143572 enhanced the downregulation of DUSP4, LRP6pS1490, MCL-1, MNK1, and PMS2. The proteins upregulated or downregulated after treatment with 5-fluorouracil, BAY1143572, or 5-fluorouracil plus BAY1143572 are listed in Supplementary Table 1.

Treatment with different doses of BAY1143572 for 4h reduced phosphorylated RNA Pol II in two EAC cell lines (eliciting a dose-dependent reduction in one of them), which supports that BAY1143572 has on-target effects against CDK9/p-TEFb (Figure 4A). MCL-1 has not been studied in the context of EAC treated with a CDK9/p-TEFb inhibitor plus a chemotherapeutic agent. Our RPPA analysis demonstrated that BAY1143572 alone and in combination with 5-fluorouracil downregulated MCL-1 in all three EAC cell lines. Therefore, we further assessed the effects of BAY1143572 on MCL-1 *in vitro*.

Treatment with 1  $\mu$ M BAY1143572 reduced MCL-1 protein expression (Figure 4A, B). To determine the role of ubiquitin-dependent MCL-1 degradation in reducing MCL-1 protein after treatment with BAY1143572, we measured the effects of BAY1143572 in cells with and without pretreatment with MG-132, an inhibitor of ubiquitin-dependent proteosomal degradation. The MCL-1 level in cells treated with BAY1143572 and MG132 was significantly higher than that in cells treated with only BAY1143572 ( $p < 0.05$ ). However, the MCL-1 level in cells treated with MG132 and BAY1143572 was significantly lower than that in cells treated with MG132 alone (Figure 4B). These findings indicate that the inhibition of proteosomal degradation partly rescues MCL-1 and that the rest of the reduction in

MCL-1 protein expression is likely due to reduced transcription (RNA level). Indeed, 4h of treatment with 1  $\mu$ M BAY1143572 reduced MCL-1 mRNA by 79.2% in SKGT4 cells, 76% in OE33 cells, and 56.4% in FLO-1 cells compared with controls (Figure 4C). ChIP assay revealed that BAY1143572 reduced the binding of HIF-1 $\alpha$  to MCL-1 in FLO-1 and OE33 cells. Compared with vehicle only, BAY1143572 significantly reduced the signal of the MCL-1 promoter bound to HIF-1 $\alpha$  antibody as compared with control, with a low signal for nonspecific binding by RbIgG (Figure 4D).

Treatment with 5-fluorouracil (5  $\mu$ M for FLO-1 and 10  $\mu$ M for SKGT4) had minimal to no effect on MCL-1 protein downregulation in FLO-1 and SKGT4 cells. Compared with either agent alone, 5-fluorouracil plus 1  $\mu$ M BAY1143572 demonstrated higher reductions of MCL-1 protein expression in FLO-1 and SKGT4 cells (Figure 5A). Treatment with 5-fluorouracil did not significantly reduce the MCL-1 mRNA level in OE33 cells and increased MCL-1 mRNA levels in FLO-1 and SKGT4 cells. Treatment with BAY1143572 and treatment with 5  $\mu$ M 5-fluorouracil plus BAY1143572 decreased MCL-1 mRNA levels. MCL-1 RNA downregulation in cells treated with BAY1143572 alone and in cells treated with BAY1143572 plus 5-fluorouracil did not differ significantly (Figure 5B).

#### *MCL-1 upregulation decreases BAY1143572's proapoptotic effects against EAC in vitro*

MCL-1 was robustly upregulated in 3 cell lines (Figure 5C). In FLO-1 cells, MCL-1 upregulation reduced apoptosis by 21% after treatment with 0.5  $\mu$ M BAY1143572, 18% after treatment with 5  $\mu$ M 5-fluorouracil, and 31% after treatment with BAY1143572 plus 5-fluorouracil as compared with the matching control ( $p < 0.01$ ). In SKGT4 cells, MCL-1 upregulation reduced apoptosis by 5% after treatment with 0.5  $\mu$ M BAY1143572, 10% after treatment with 5-fluorouracil, and 8% after treatment with BAY1143572 plus 5-fluorouracil as compared with the matching control ( $p < 0.01$ ; Figure 5D).

#### *High MCL-1 expression in pretreatment tumor cells predicts shorter overall survival in patients with locoregional EAC*

The median *H*-score of MCL-1 expression in tumor cells in pretreatment samples was 40

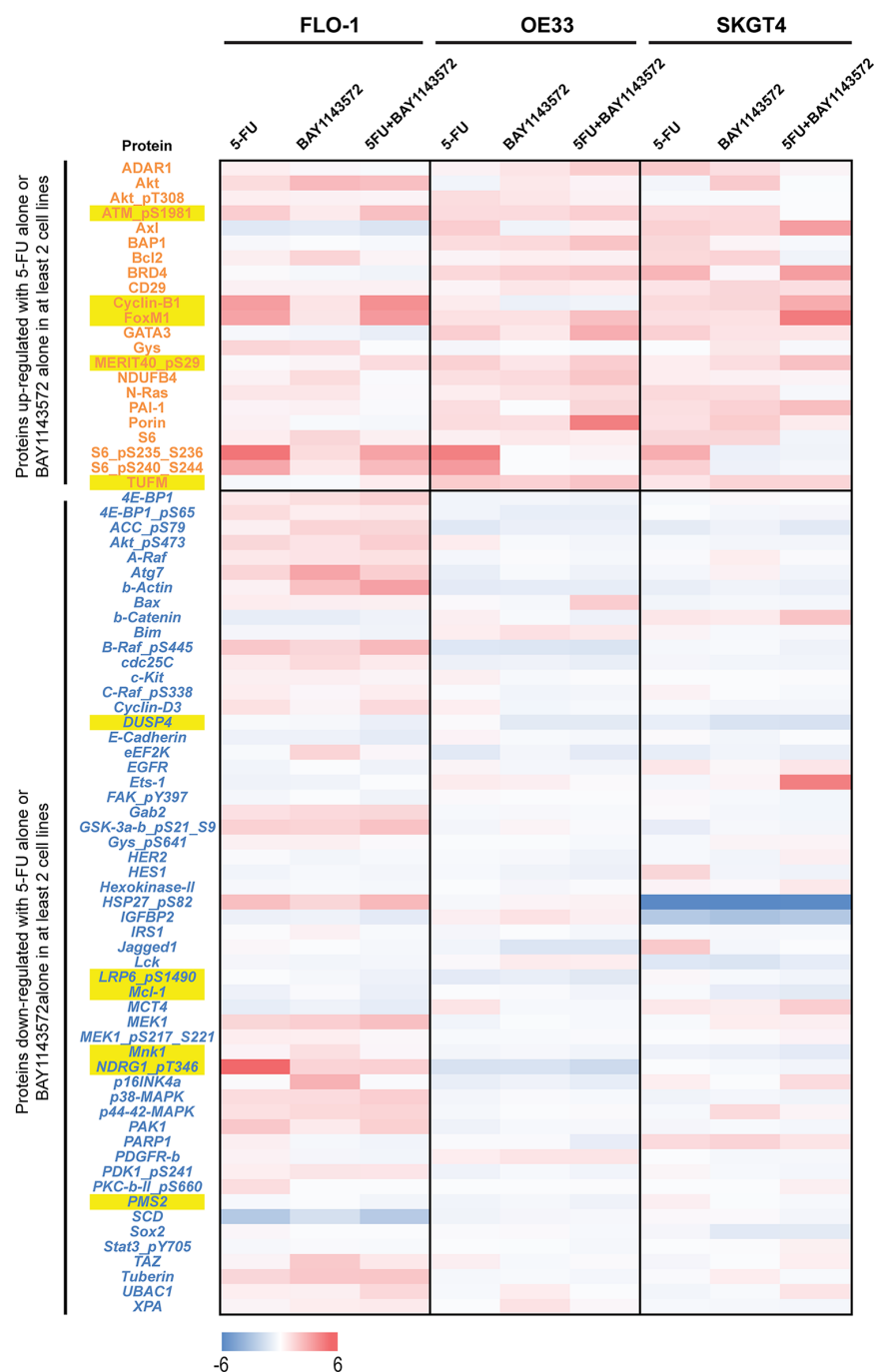


**Figure 3. Effects of BAY1143572 with or without 5-fluorouracil on the proteomics profile of esophageal adenocarcinoma.** Lysates from cells treated with 1  $\mu$ M BAY1143572 with or without 5-fluorouracil (10  $\mu$ M for OE33 and SKGT4 cells, 5  $\mu$ M for FLO-1 cells) for 30h were subjected to reverse phase protein array [RPPA] analysis. Protein-level data were normalized for protein loading and transformed to linear values. The heat map indicates the difference in the linear values between control (vehicle treatment only) and the treatment groups. The blue indicating negative (<0) difference between control and the treatment group indicating reduction in the protein and red indicating positive (>0) difference between control and the treatment group indicating increase in the protein expression. Proteins in red font are upregulated oncoproteins after treatment with either 5-fluorouracil or BAY1143572 in at least two cell lines. Proteins in blue font are downregulated oncoproteins after treatment with either 5-fluorouracil or BAY1143572 in at least two cell lines. Yellow highlighted proteins are those with higher upregulation or downregulation after treatment with BAY1143572 plus 5-fluorouracil as compared with single-agent treatment in at least two cell lines.

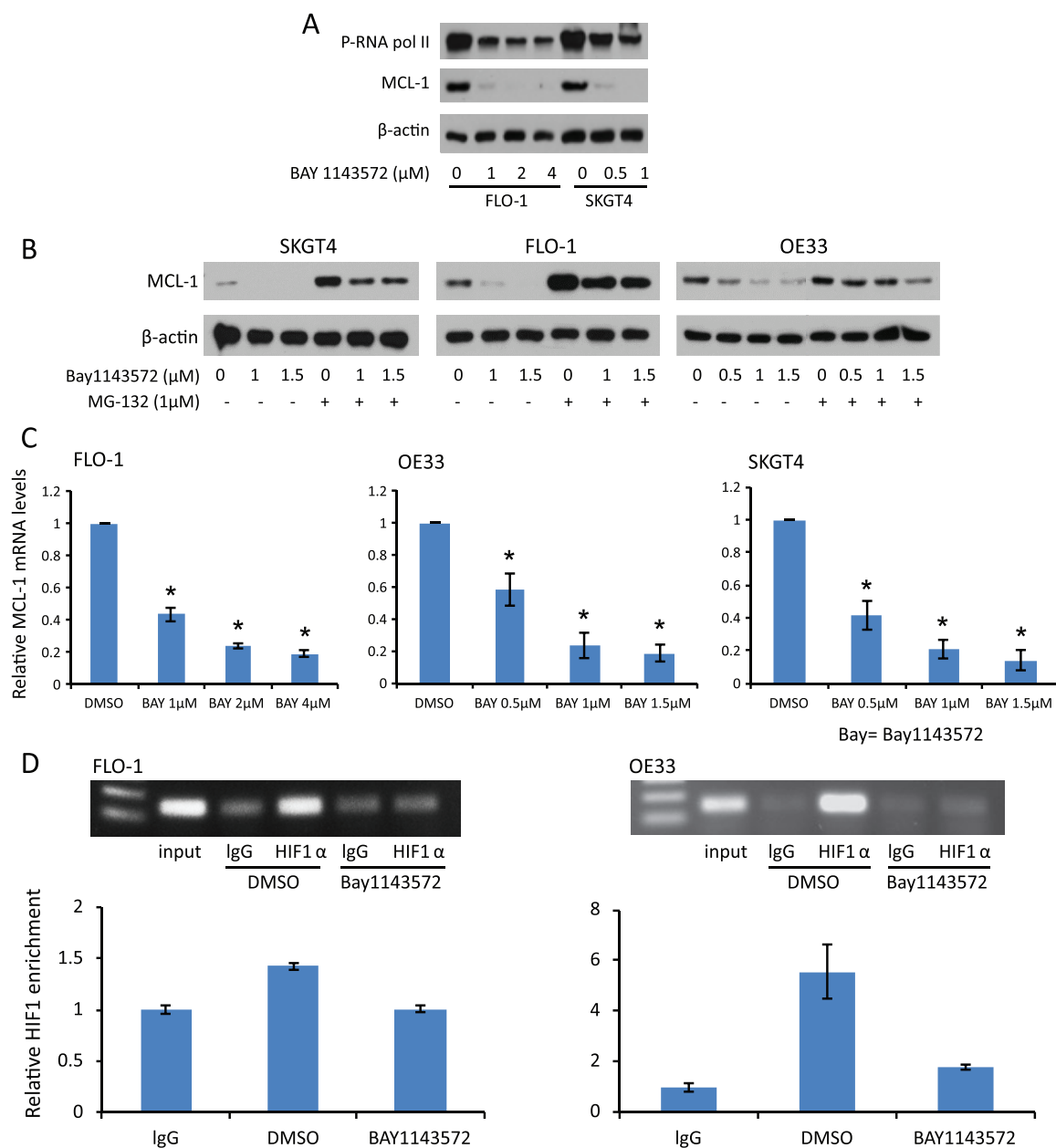


**Figure 4. Effects of BAY1143572 on MCL-1 protein and RNA levels in *in vitro* models of esophageal adenocarcinoma.** [A] Cells were treated with BAY1143572 at the indicated doses for 4 h. The phosphorylation of RNAPII and the expression of MCL-1 were examined by Western blotting. [B] Cells were treated with 1  $\mu$ M BAY1143572 for 4 h after pretreatment with or without MG-123 for 1 h. MCL-1 protein levels were assessed by Western blotting. [C] MCL-1 mRNA levels were measured by quantitative real-time polymerase chain reaction (qPCR) after treatment with the indicated doses of BAY1143572 for 4 h. [D] Chromatin immunoprecipitation (ChIP) was used to assess the binding of HIF-1 $\alpha$  to the MCL-1 promoter in FLO-1 and OE33 cells treated with 1  $\mu$ M BAY1143572 or vehicle only for 4 h. qPCR results show the means of experiments performed in triplicate for each treatment condition. Similar results were observed in two independent experiments.

(range, 0–250). Higher MCL-1 *H*-score ( $H \geq 40$ ) correlated with higher pathologic tumor stage (pT3–T4). There was no significant difference in other clinical and pathologic variables between patients whose tumors had low MCL-1

expression ( $H < 40$ ; Figure 6A) and those whose tumors had high MCL-1 expression ( $H \geq 40$ ; Figure 6B), as shown in Supplementary Table 2. Kaplan–Meier analysis showed that patients with high MCL-1 expression had significantly worse

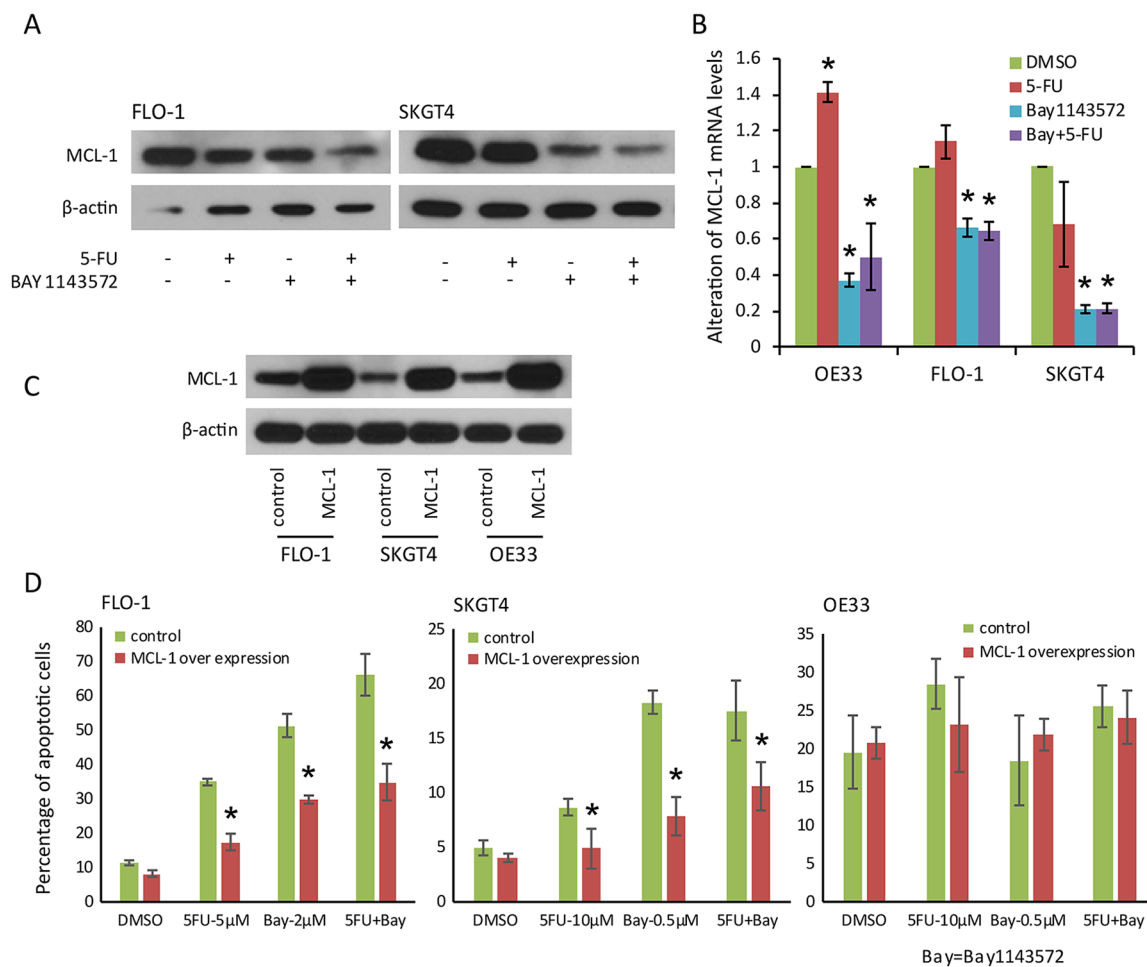


**Figure 5. Effects of BAY1143572 plus 5-fluorouracil on MCL-1 protein and RNA levels in *in vitro* models of esophageal adenocarcinoma.** (A) Lysates from cells treated with 1 µM BAY1143572 with or without 5-fluorouracil (10 µM for SKGT4 cells, 5 µM for FLO-1 cells) for 4 h were subjected to Western blotting for MCL-1. (B) Cells were treated with 1 µM BAY1143572 with or without 5-fluorouracil (10 µM for OE33 and SKGT4 cells, 5 µM for FLO-1 cells) for 4 h, and their MCL-1 mRNA levels were measured by quantitative real-time polymerase chain reaction (qPCR). Data are the means ± standard error (SE) of three independent experiments. (C) Western blot of esophageal adenocarcinoma cell lines with stable overexpression of MCL-1. (D) Cells with or without MCL-1 overexpression were treated with 5-fluorouracil and/or BAY1143572 at the indicated doses and then stained with Annexin V-FITC and propidium iodide. Apoptosis was analyzed by flow cytometry. Data are the means ± SE of three independent experiments. \**p* < 0.05 compared with control cells.

and overall and recurrence (or time to death) survival, than patients with low MCL-1 expression did (Figure 6C and D). The median overall survival duration of patients with tumors with low MCL-1 expression (65 months) was significantly longer than that of patients with tumors with high MCL-1 expression (30 months), *p* = 0.012). In the Cox regression univariate analysis, higher pathologic nodal stage, receipt of therapy for recurrence, and high tumor cell MCL-1 expression were associated with shorter overall survival. In the multivariate analysis, high tumor cell

MCL-1 expression and receipt of therapy for recurrence were associated with shorter overall survival, whereas pathologic nodal stage demonstrated a trend towards an association with shorter overall survival (Table 1). The median recurrence-free (or time to death) survival duration of patients with tumors with low MCL-1 expression (60 months) was significantly longer than that of patients with tumors with high MCL-1 expression (18 months, *p* = 0.008). In the Cox regression univariate and multivariate analyses, higher pathologic nodal stage and high tumor cell MCL-1

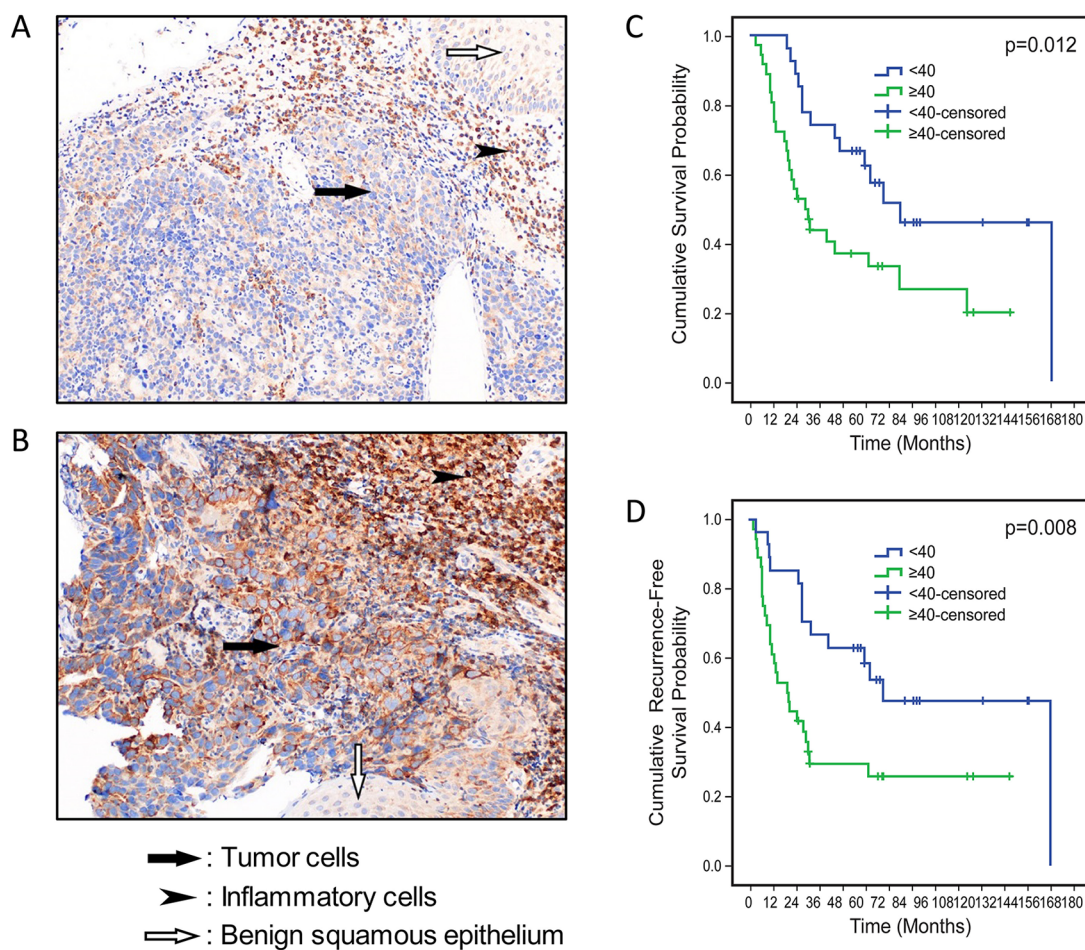


**Figure 6. Correlation of MCL-1 protein expression in pretreatment tumor cells with overall survival and recurrence free survival of patients with locoregional esophageal adenocarcinoma treated with neoadjuvant chemoradiation and surgery.** (A) Photomicrograph of MCL-1 immunohistochemical staining of a pretreatment tumor with low MCL-1 expression (200 $\times$  magnification). (B) Photomicrograph of MCL-1 immunohistochemical staining of a pretreatment tumor with high MCL-1 expression (200 $\times$  magnification). (C) Kaplan-Meier overall survival curves for patients with high tumor MCL-1 expression and patients with low tumor MCL-1 expression. (D) Kaplan-Meier recurrence free (or time to death) survival curves for patients with high tumor MCL-1 expression and patients with low tumor MCL-1 expression.

expression were associated with shorter recurrence-free (or time to death) survival (Table 2).

### Discussion

The results of our *in vitro* and xenograft experiments demonstrate that the inhibition of CDK9/p-TEFb by BAY1143572 alone or in combination with 5-fluorouracil is effective against EAC. In this study, BAY1143572's dose-dependent effects on cell proliferation and its narrow range of  $IC_{50}$  in six EAC cell lines suggest that CDK9 inhibitors have efficacy against EAC.

The findings of the present study and a previous study<sup>7</sup> demonstrate that three CDK inhibitors

with predominant CDK9 inhibitory effects, BAY1143572, flavopiridol, and CAN508, have similar antitumorigenic effects against EAC. These drugs also downregulate the phosphorylation of RNA Pol II and transcriptionally downregulate MCL-1 by inhibiting HIF1- $\alpha$  binding to the MCL-1 promoter in EAC. These results indicate that BAY1143572 has on-target effects against CDK9 in EAC. BAY1143572's higher specificity against CDK9/p-TEFb and strong efficacy *in vitro* and in murine xenografts of EAC support a study investigating the role of BAY1143572 as an adjunct to chemotherapy or radiotherapy in EAC.

5-fluorouracil is one of the most widely used agents in bimodality and trimodality neoadjuvant therapy

**Table 1.** Cox regression analysis correlating MCL-1 expression *H*-score and other clinicopathologic variables with patients' overall survival.

	Univariate analysis				Multivariate analysis			
	<i>p</i>	Hazard ratio	95% confidence interval		<i>p</i>	Hazard ratio	95% confidence interval	
Age	0.50	0.99	0.95	1.02				
Histology grade (poor or undiff)	0.63	0.85	0.44	1.63				
ypT stage (pT3–T4)	0.36	1.38	0.69	2.74				
ypN stage (pN1–3)	0.01	2.41	1.21	4.79	0.23	1.57	0.75	3.29
Pathologic response (P2)	0.13	1.71	0.86	3.39	0.28	1.49	0.73	3.06
Therapy for recurrence or progression	0.00	3.99	1.99	8.01	0.00	3.56	1.73	7.34
MCL-1 <i>H</i> -score $\geq 40$	0.02	2.32	1.18	4.56	0.01	2.38	1.19	4.72

**Table 2.** Cox regression analysis correlating MCL-1 expression *H*-score and other clinicopathologic variables with patients' recurrence-free (or time to death) survival.

	Univariate analysis				Multivariate analysis			
	<i>p</i>	Hazard ratio	95% confidence interval		<i>p</i>	Hazard ratio	95% confidence interval	
Age	0.16	0.97	0.94	1.01	0.28	0.98	0.95	1.02
Histology grade (poor or undiff)	0.89	1.05	0.55	1.99				
ypT stage (ypT3–T4)	0.18	1.59	0.80	3.14	0.60	0.80	0.35	1.84
ypN stage (pN1–3)	0.03	2.07	1.06	4.04	0.04	2.16	1.02	4.57
Pathologic response (P2)	0.33	1.40	0.71	2.77				
MCL-1 <i>H</i> -score $\geq 40$	0.01	2.42	1.23	4.75	0.01	2.42	1.23	4.75

as well postoperative chemotherapy in patients with esophageal or gastroesophageal junction adenocarcinoma.<sup>1,26–28</sup> However, few studies have assessed the role of targeted agents in combination with 5-fluorouracil-based chemotherapy or chemoradiotherapy in EAC. Most of these studies are limited to targeted agents whose efficacy has already been established in other solid tumors.<sup>29–34</sup> Ours is the first study to demonstrate synergy between a CDK9 inhibitor and 5-fluorouracil *in vitro* and in inhibiting the growth of murine xenografts of EAC. The BAY1143572 dose required to achieve synergy varied across cell lines; a dose lower than the IC<sub>50</sub> was required for OE33 and FLO-1 cells, whereas a dose close to the IC<sub>50</sub> was

required for SKGT4 cells, indicating a heterogeneity of response to BAY1143572 in combination with 5-fluorouracil. Unlike synergy in proliferation in all three EAC cell lines, BAY1143572 significantly enhanced the effects of 5-fluorouracil-induced apoptosis in FLO1 and SKGT4 cells but not in OE33 cells. These findings suggest heterogeneity in the synergistic effects of these agents across different EAC cells. It is likely that effects of BAY1143572 with and without 5-fluorouracil in OE33 and ESO26 are by different mechanism such as cell cycle arrest in G1 or G2-M phase.

In xenograft experiments, synergy between 15 mg/kg BAY1143572 and 5-fluorouracil was evident in

most ESO-26 xenografts on day 21 and in most FLO-1 xenografts on day 40. BAY1143572 alone could inhibit the growth of most FLO-1 xenografts until 21 days after treatment initiation. That the inhibitory effects of BAY1143572 plus 5-fluorouracil were longer than those of BAY1143572 alone in FLO-1 xenografts supports the synergy between BAY1143572 and 5-fluorouracil.

Although 5-fluorouracil did not alter MCL-1 RNA and protein expression, the combination of 5-fluorouracil and BAY1143572 enhanced the downregulation of the MCL-1 protein *in vitro*, indicating that these two agents have synergy in downregulating MCL-1. In addition, 5-fluorouracil enhanced the BAY1143572-induced downregulation of MCL-1 protein but not that of MCL-1 mRNA, indicating that MCL-1 modification is at the post-transcription or post-translational stage by the combination of these agents. BAY1143572 alone and the combination of BAY1143572 and 5-fluorouracil likely have different mechanisms of MCL-1 downregulation, which provides additional support of the relevance of MCL-1 as a likely target of the combination treatment. Compared with control (nonamplified MCL-1), MCL-1 upregulation induced less apoptosis after treatment with 5-fluorouracil and/or BAY1143572 in two EAC cell lines, indicating that the apoptosis mediated by BAY1143572 and 5-fluorouracil depends on MCL-1.

One limitation of the present study was the lack of validation of the synergistic effects of BAY1143572 and 5-fluorouracil on MCL-1 in xenografts. MCL-1, a protein with a short half-life, is regulated by multiple mechanisms. At the end of the experiments, xenografts were unlikely to have reduced MCL-1 levels owing to the transient and reversible effects of CDK9 inhibition on MCL-1 and the normalization of MCL-1 levels by other compensatory mechanisms.<sup>35–37</sup> MCL-1 levels in xenografts should be measured immediately after CDK9 inhibitor treatment to demonstrate the effects of CDK9 inhibitors on MCL-1 in xenografts.

MCL-1 is a ubiquitous protein whose expression pattern in EAC is not known. For this reason and to obtain an MCL-1 *H*-score cut-off that can be used to classify patients as those with good *versus* those with poor response to neoadjuvant chemoradiation, we used the *H*-score method and median level of the *H*-score as the cut-off. We found that MCL-1 expression in patients' tumor cells was correlated with survival outcomes, further supporting the substantial role MCL-1 has in

EAC biology and behavior. Our results showing that MCL-1 expression is at least as significant as established prognostic factors such as nodal stage. This finding indicates that further studies investigating MCL-1 as predictor of neoadjuvant therapy response in patients with localized EAC are warranted.

Our RPPA data showing the upregulation of ATMpS1981<sup>38</sup> and FOX-M1<sup>39,40</sup> indicate that the DNA damage repair mechanism is a likely mechanism of synergy between BAY1143572 and 5-fluorouracil. The downregulation of LGRP6pS1490 and MNK1 suggest a synergistic role of BAY1143572 and 5-fluorouracil in the Wnt pathway and/or MAP kinase pathway<sup>41</sup> in EAC.

In conclusion, the present study provides ample preclinical data supporting a clinical trial of BAY1143572 alone or in combination with 5-fluorouracil in patients with EAC, using MCL-1 as a potential predictor of response to these therapies.

### Acknowledgements

We thank Joe Munch in MD Anderson's Department of Scientific Publications for editing the manuscript and Kim-Anh Vu in MD Anderson's Department of Anatomic Pathology for helping with the figures.

### Author contributions

DM, ZT, AMC, and OV conceived and designed the study. ZT, AM, OV, RD, AV, VP, RK, BM, LMS, JRC, and WLH collected and analyzed the data. DM, ZT, AM, OV, SHL, JAA, MB, SK, and SK wrote and edited the manuscript. All authors approved the final manuscript.

### Conflict of interest statement

The authors declare that there is no conflict of interest.

### Funding

The author(s) disclosed receipt of the following financial support for the research, authorship, and/or publication of this article: This work was funded in part by an Independent Investigator Award from the Cancer Prevention and Research Institute of Texas (award number RP140515, to Dr. Dipen Maru). Part of this research was performed in MD Anderson's Flow Cytometry and Cellular Imaging Facility, which is supported in part by the National Institutes of Health through MD Anderson's Cancer Center Support (grant number CA016672).

**Availability of data and material**

All datasets and materials used and/or analyzed during the current study are available from the corresponding author on reasonable request.

**ORCID iD**

Dipen M. Maru  <https://orcid.org/0000-0002-9134-7709>

**Supplemental material**

Supplemental material for this article is available online.

**References**

1. Ychou M, Boige V, Pignon JP, *et al.* Perioperative chemotherapy compared with surgery alone for resectable gastroesophageal adenocarcinoma: an FNCLCC and FFCO multicenter phase III trial. *J Clin Oncol* 2011; 29: 1715–1721.
2. van Hagen P, Hulshof MC, van Lanschot JJ, *et al.* Preoperative chemoradiotherapy for esophageal or junctional cancer. *N Engl J Med* 2012; 366: 2074–2084.
3. Shapiro J, van Lanschot JJ, Hulshof MC, *et al.* Neoadjuvant chemoradiotherapy plus surgery versus surgery alone for oesophageal or junctional cancer (CROSS): long-term results of a randomised controlled trial. *Lancet Oncol* 2015; 16: 1090–1098.
4. Bang YJ, Van Cutsem E, Feyereislova A, *et al.* Trastuzumab in combination with chemotherapy versus chemotherapy alone for treatment of HER2-positive advanced gastric or gastro-oesophageal junction cancer (ToGA): a phase 3, open-label, randomised controlled trial. *Lancet* 2010; 376: 687–697.
5. Waddell T, Chau I, Cunningham D, *et al.* Epirubicin, oxaliplatin, and capecitabine with or without panitumumab for patients with previously untreated advanced oesophagogastric cancer (REAL3): a randomised, open-label phase 3 trial. *Lancet Oncol* 2013; 14: 481–489.
6. Crosby T, Hurt CN, Falk S, *et al.* Long-term results and recurrence patterns from SCOPE-1: a phase II/III randomised trial of definitive chemoradiotherapy +/- cetuximab in oesophageal cancer. *Br J Cancer* 2017; 116: 709–716.
7. Tong Z, Chatterjee D, Deng D, *et al.* Antitumor effects of cyclin dependent kinase 9 inhibition in esophageal adenocarcinoma. *Oncotarget* 2017; 8: 28696–28710.
8. Chen XX, Xie FF, Zhu XJ, *et al.* Cyclin-dependent kinase inhibitor dinaciclib potently synergizes with cisplatin in preclinical models of ovarian cancer. *Oncotarget* 2015; 6: 14926–14939.
9. Rathkopf D, Dickson MA, Feldman DR, *et al.* Phase I study of flavopiridol with oxaliplatin and fluorouracil/leucovorin in advanced solid tumors. *Clin Cancer Res* 2009; 15: 7405–7411.
10. Walsby E, Pratt G, Shao H, *et al.* A novel Cdk9 inhibitor preferentially targets tumor cells and synergizes with fludarabine. *Oncotarget* 2014; 5: 375–385.
11. Morales F and Giordano A. Overview of CDK9 as a target in cancer research. *Cell Cycle* 2016; 15: 519–527.
12. Kumar SK, LaPlant B, Chng WJ, *et al.* Dinaciclib, a novel CDK inhibitor, demonstrates encouraging single-agent activity in patients with relapsed multiple myeloma. *Blood* 2015; 125: 443–448.
13. Stephenson JJ, Nemunaitis J, Joy AA, *et al.* Randomized phase 2 study of the cyclin-dependent kinase inhibitor dinaciclib (MK-7965) versus erlotinib in patients with non-small cell lung cancer. *Lung Cancer* 2014; 83: 219–223.
14. Dickson MA, Shah MA, Rathkopf D, *et al.* A phase I clinical trial of FOLFIRI in combination with the pan-cyclin-dependent kinase (CDK) inhibitor flavopiridol. *Cancer Chemother Pharmacol* 2010; 66: 1113–1121.
15. Heath EI, Bible K, Martell RE, *et al.* A phase 1 study of SNS-032 (formerly BMS-387032), a potent inhibitor of cyclin-dependent kinases 2, 7 and 9 administered as a single oral dose and weekly infusion in patients with metastatic refractory solid tumors. *Invest New Drugs* 2008; 26: 59–65.
16. Morris DG, Bramwell VH, Turcotte R, *et al.* A phase II study of flavopiridol in patients with previously untreated advanced soft tissue sarcoma. *Sarcoma* 2006; 2006: 64374.
17. Narita T, Ishida T, Ito A, *et al.* Cyclin-dependent kinase 9 is a novel specific molecular target in adult T-cell leukemia/lymphoma. *Blood* 2017; 130: 1114.
18. Lucking U, Scholz A, Lienau P, *et al.* Identification of atuvaciclib (BAY 1143572), the first highly selective, clinical PTEFb/CDK9 inhibitor for the treatment of cancer. *ChemMedChem* 2017; 12: 1776–1793.
19. Scholz A, Oellerich T, Hussain A, *et al.* BAY 1143572: a first-in-class, highly selective, potent and orally available inhibitor of PTEFb/CDK9 currently in phase I, inhibits MYC and shows convincing anti-tumor activity in multiple xenograft models by the induction of apoptosis. AACR 106th Annual Meeting, 2015, New Orleans, LA.



20. Chou TC. Drug combination studies and their synergy quantification using the Chou-Talalay method. *Cancer Res* 2010; 70: 440–446.
21. Chou TC. Theoretical basis, experimental design, and computerized simulation of synergism and antagonism in drug combination studies. *Pharmacol Rev* 2006; 58: 621–681.
22. D'Alessandro R, Refolo MG, Lippolis C, *et al.* Strong enhancement by IGF1-R antagonists of hepatocellular carcinoma cell migration inhibition by Sorafenib and/or vitamin K1. *Cell Oncol (Dordr)* 2018; 41: 283–296.
23. Rozati S, Cheng PF, Widmer DS, *et al.* Romidepsin and azacitidine synergize in their epigenetic modulatory effects to induce apoptosis in CTCL. *Clin Cancer Res* 2016; 22: 2020–2031.
24. Tibes R, Qiu Y, Lu Y, *et al.* Reverse phase protein array: validation of a novel proteomic technology and utility for analysis of primary leukemia specimens and hematopoietic stem cells. *Mol Cancer Ther* 2006; 5: 2512–2521.
25. Wang Y, Liu H, Diao L, *et al.* Hsp90 inhibitor ganetespib sensitizes non-small cell lung cancer to radiation but has variable effects with chemoradiation. *Clin Cancer Res* 2016; 22: 5876–5886.
26. Conroy T, Galais MP, Raoul JL, *et al.* Definitive chemoradiotherapy with FOLFOX versus fluorouracil and cisplatin in patients with oesophageal cancer (PRODIGE5/ACCORD17): final results of a randomised, phase 2/3 trial. *Lancet Oncol* 2014; 15: 305–314.
27. Mariette C, Dahan L, Mornex F, *et al.* Surgery alone versus chemoradiotherapy followed by surgery for stage I and II esophageal cancer: final analysis of randomized controlled phase III trial FFCD 9901. *J Clin Oncol* 2014; 32: 2416–2422.
28. Tepper J, Krasna MJ, Niedzwiecki D, *et al.* Phase III trial of trimodality therapy with cisplatin, fluorouracil, radiotherapy, and surgery compared with surgery alone for esophageal cancer: CALGB 9781. *J Clin Oncol* 2008; 26: 1086–1092.
29. Catenacci DVT, Tebbutt NC, Davidenko I, *et al.* Rilotumumab plus epirubicin, cisplatin, and capecitabine as first-line therapy in advanced MET-positive gastric or gastro-oesophageal junction cancer (RILOMET-1): a randomised, double-blind, placebo-controlled, phase 3 trial. *Lancet Oncol* 2017; 18: 1467–1482.
30. Enzinger PC, Burtneis BA, Niedzwiecki D, *et al.* CALGB 80403 (Alliance)/E1206: a randomized phase II study of three chemotherapy regimens plus cetuximab in metastatic esophageal and gastroesophageal junction cancers. *J Clin Oncol* 2016; 34: 2736–2742.
31. Hecht JR, Bang YJ, Qin SK, *et al.* Lapatinib in combination with capecitabine plus oxaliplatin in human epidermal growth factor receptor 2-positive advanced or metastatic gastric, esophageal, or gastroesophageal adenocarcinoma: TRIO-013/LOGiC—a randomized phase III trial. *J Clin Oncol* 2016; 34: 443–451.
32. Moehler M, Gepfner-Tuma I, Maderer A, *et al.* Sunitinib added to FOLFIRI versus FOLFIRI in patients with chemorefractory advanced adenocarcinoma of the stomach or lower esophagus: a randomized, placebo-controlled phase II AIO trial with serum biomarker program. *BMC Cancer* 2016; 16: 699.
33. Pant S, Patel M, Kurkjian C, *et al.* A phase II study of the c-met inhibitor tivantinib in combination with folfox for the treatment of patients with previously untreated metastatic adenocarcinoma of the distal esophagus, gastroesophageal junction, or stomach. *Cancer Invest* 2017; 35: 463–472.
34. Yoon HH, Bendell JC, Braiteh FS, *et al.* Ramucirumab combined with FOLFOX as front-line therapy for advanced esophageal, gastroesophageal junction, or gastric adenocarcinoma: a randomized, double-blind, multicenter phase II trial. *Ann Oncol* 2016; 27: 2196–2203.
35. Liu H, Yang J, Yuan Y, *et al.* Regulation of Mcl-1 by constitutive activation of NF-kappaB contributes to cell viability in human esophageal squamous cell carcinoma cells. *BMC Cancer* 2014; 14: 98.
36. Hsieh MJ, Hsieh YH, Lin CW, *et al.* Transcriptional regulation of Mcl-1 plays an important role of cellular protective effector of vincristine-triggered autophagy in oral cancer cells. *Expert Opin Ther Targets* 2015; 19: 455–470.
37. Hu J, Dang N, Menu E, *et al.* Activation of ATF4 mediates unwanted Mcl-1 accumulation by proteasome inhibition. *Blood* 2012; 119: 826–837.
38. Bakkenist CJ and Kastan MB. DNA damage activates ATM through intermolecular autophosphorylation and dimer dissociation. *Nature* 2003; 421: 499–506.
39. Tan Y, Raychaudhuri P and Costa RH. Chk2 mediates stabilization of the FoxM1 transcription factor to stimulate expression of DNA repair genes. *Mol Cell Biol* 2007; 27: 1007–1016.
40. Khongkow P, Karunarathna U, Khongkow M, *et al.* FOXM1 targets NBS1 to regulate DNA damage-induced senescence and epirubicin resistance. *Oncogene* 2014; 33: 4144–4155.
41. Hou S, Du P, Wang P, *et al.* Significance of MNK1 in prognostic prediction and chemotherapy development of epithelial ovarian cancer. *Clin Transl Oncol* 2017; 19: 1107–1116.